

**ACCGE-
20**

OMVPE-17

August 2-7, 2015

Big Sky, Montana, USA

CHARACTERIZATION OF CdZnTe SINGLE CRYSTALS GROWN UNDER DIFFERENT CADMIUM OVERPRESSURES

Ouloide Yannick Goue¹, Balaji Raghothomachar¹, Michael Dudley¹, Ching Hua Su²

1. Materials Science and Engineering Dpt, Stony Brook University, NY 11794-2275 USA

2. NASA/Marshall space flight center, Huntsville, Al 35812 USA

OUTLINE

- Motivation
- Formation of Te inclusions/precipitate
- Crystal Growth of CdZnTe
- Synchrotron X-ray Topography Technique
- Correlation between synchrotron white beam X-ray topography (SXRT) and transmission infrared microscopy
- Effect of Cd reservoir temperature on Te inclusion density
- Summary

MOTIVATION

CdZnTe has gradually become a choice material for radiation detectors due to its:

- ❑ Direct wide band gap (1.5-2.3 eV) \Rightarrow High bulk resistivity
- ❑ Large cross-section \Rightarrow Good photoelectric absorption
- ❑ High energy resolution comparable to high quality Ge (0.5% at 662 keV) and high spatial resolution ($\sim\mu\text{m}$) for imaging
- ❑ Ability to operate at room temperature \Rightarrow no cooling required

Current CdZnTe Applications include

- ❑ National security (nuclear waste management, nonproliferation of nuclear materials,...)
- ❑ Medical imaging (PET and CT scanners, medical probes,...)
- ❑ Basic science (astrophysics, γ -spectrometer, synchrotron X-ray research,...)
- ❑ Industrial imaging (X-ray and γ -ray cameras,...)
- ❑ Electro-optic modulators and laser windows

Comparison of CdZnTe with detector materials

Average atomic #	CdZnTe	Ge	Si
	49.1	32	14
Density (g/cm ³)	5.78	5.32	2.33
Resistivity (W-cm)	10^{10}	47	2.3×10^5

bone densitometer



<http://www.megamedicals.com/mm-x010-bone-densitometry.htm>



Miniaturized probe for radioguided surgery

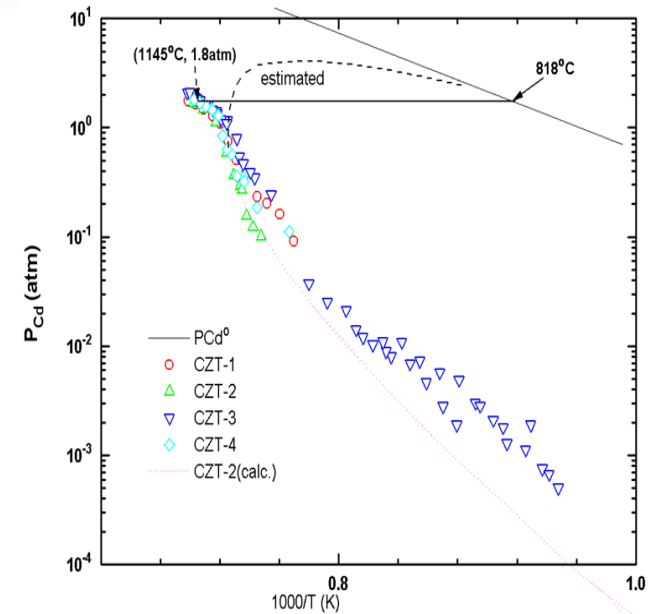
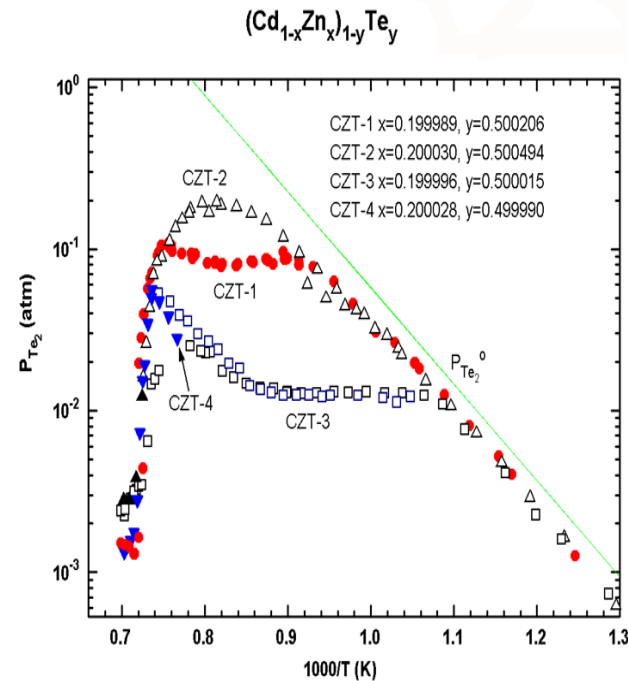
<http://precise-healthcare.com/CrystalPhotonics.aspx>

FORMATION OF Te INCLUSION/PRECIPTATES

- Te precipitates (\sim nm order) form from the retrograde solid solubility effect in CdZnTe during rapid cooling from high temperature, whereas Te inclusions (\sim μ m order) result from trapping of the excess Te at growth interface because of fluctuation in growth conditions (e.g. temperature, pressure)
- These secondary phases (Te inclusions/precipitates) reduce infrared transmission and also affect detector performance (e.g. by reducing carrier lifetime)

⇒ **How to inhibit/prevent the formation of these secondary phase Te particles???**

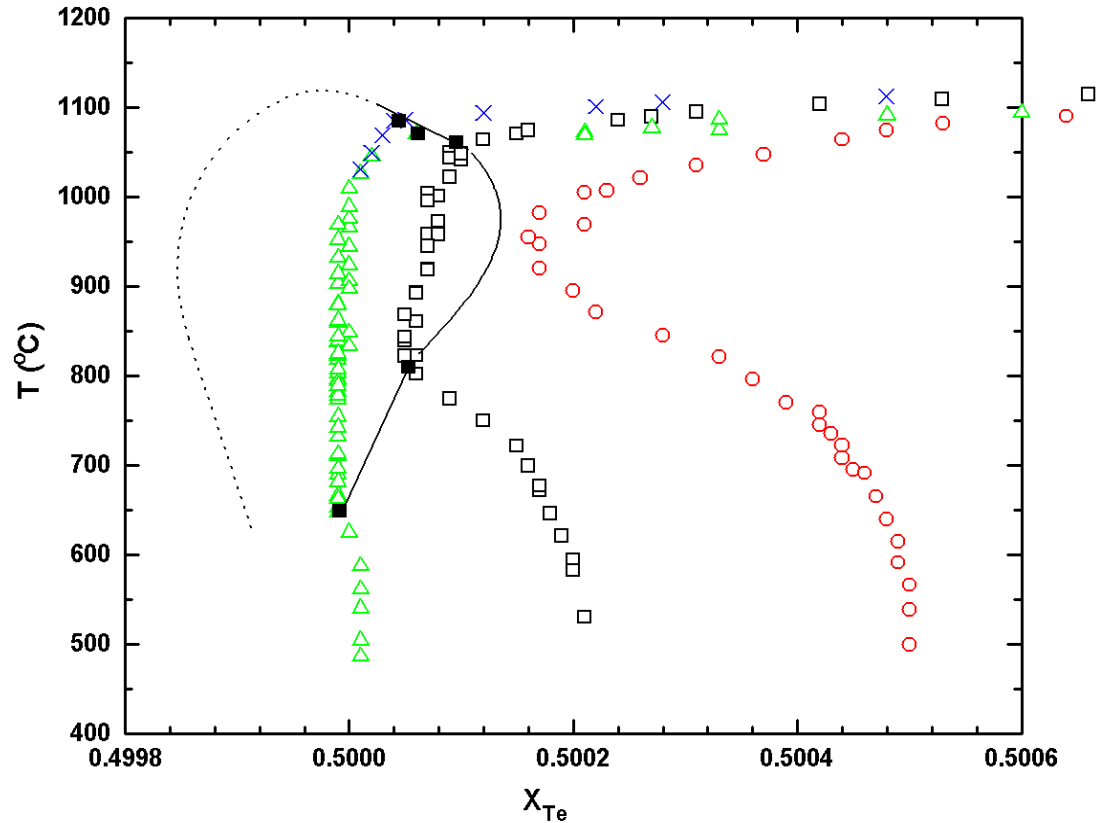
⇒ ⇒ **A proposed solution is to use saturated Cd vapor pressure!!!**



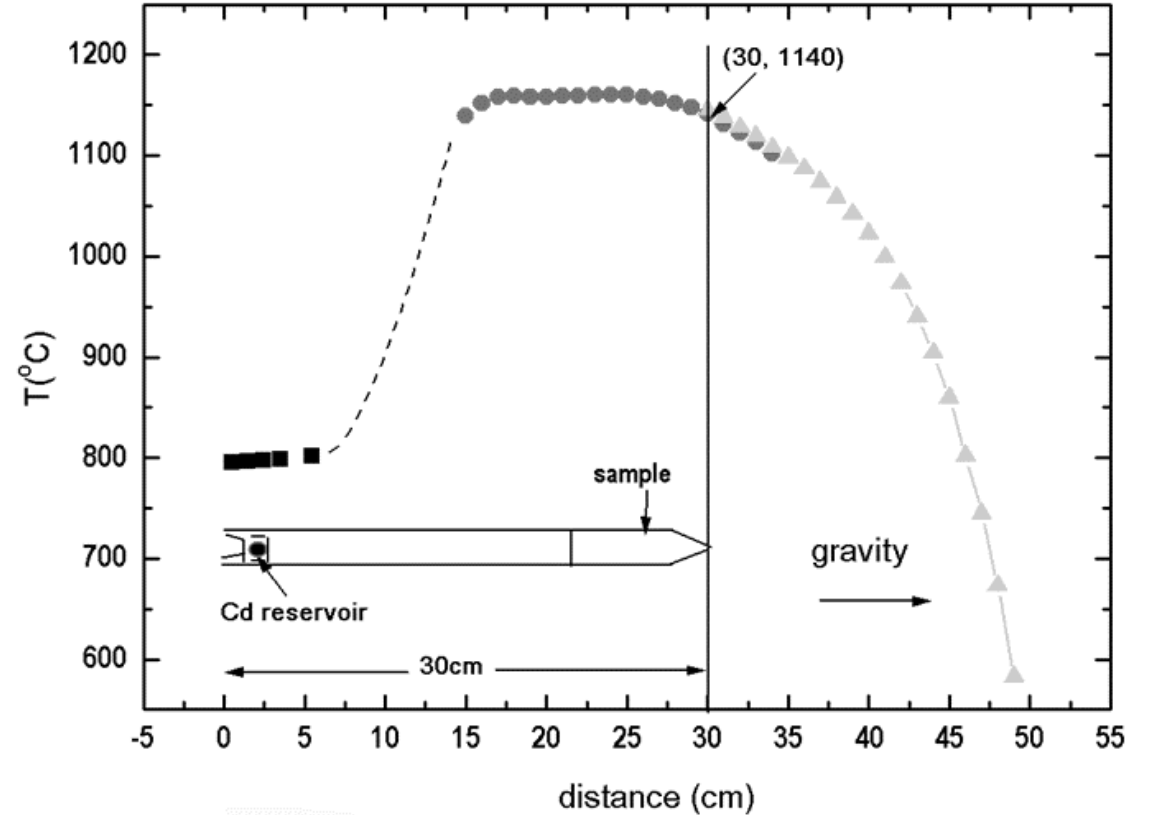
Partial pressures of Te_2 (left) and Cd (right) for four samples of $\text{Cd}_{0.8}\text{Zn}_{0.2}\text{Te}$ with different Te contents have been measured [1].

One implication from the partial pressure measurements is that the partial pressures of Te_2 and Cd over the melt at growth temperature (1150°C) differ by 3 orders of magnitude. Therefore, an initially stoichiometric sample will be Te-rich during growth because more Cd is lost to the free volume. A Cd reservoir of 818°C will provide the Cd in the vapor phase and maintain the melt at stoichiometry.

[1] Ching-Hua Su and S. L. Lehoczky, "Melt growth of high-resistivity CdZnTe crystals by controlling Cd over-pressures", J. Crystal Growth Vol. 319, 4-7 (2011).



The homogeneity range of $\text{Cd}_{0.8}\text{Zn}_{0.2}\text{Te}$ solid solution determined from partial pressure measurements. Solid squares are the solubility limits at Te-saturated condition. The maximum limit is less than 0.50016. There are no data points on the Cd-rich region and dotted line is arbitrarily drew.

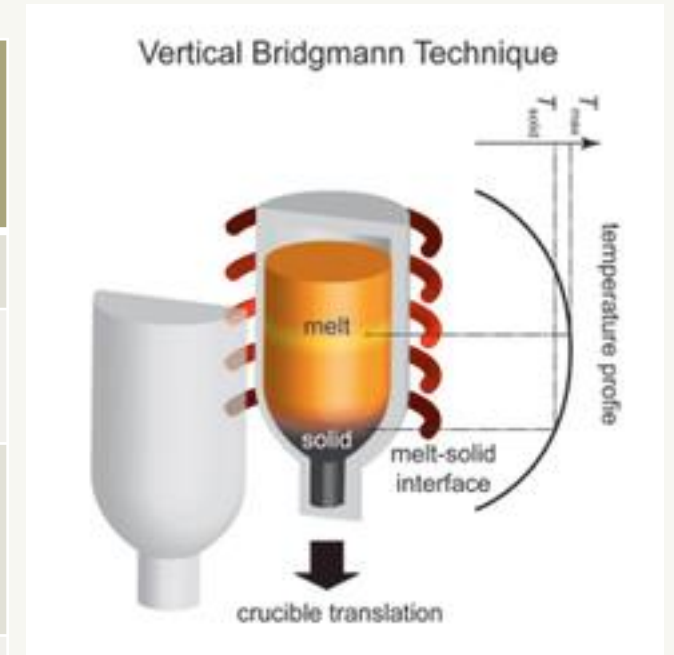


The thermal profile and the initial ampoule position for a typical crystal growth by vertical directional solidification with controlled Cd over-pressure.

CRYSTAL GROWTH OF CDZNTE

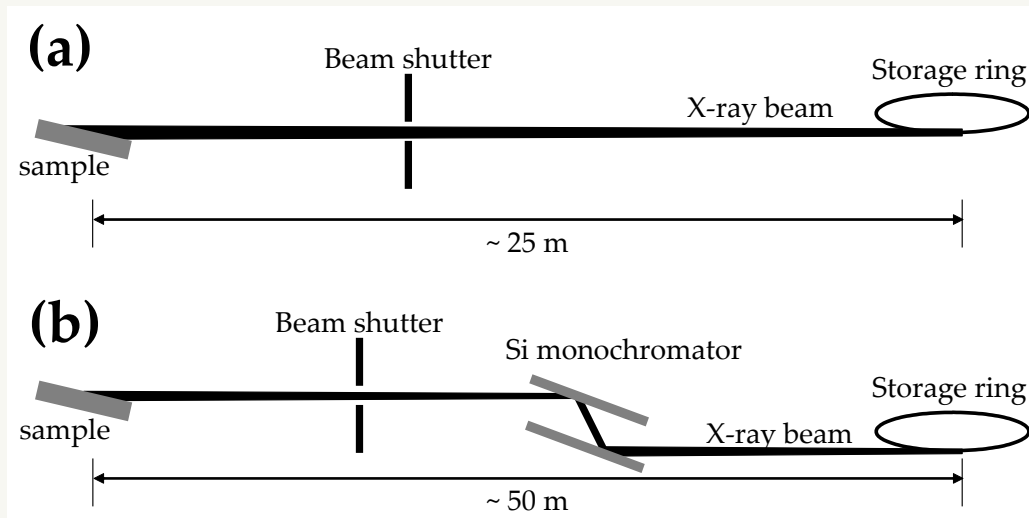
CdZnTe boules were grown by vertical directional solidification method, and subjected to different Cd

Sample	Start material	T (°C) Cd reservoir	Growth time (hr)	Sample cooling time (hr)	Cd reservoir cooling rate during growth
2G-30	Batch #2	785	120	144	80°C in last 60 hr
2G-31	Batch #2	800	125	96	65°C in last 60 hr, quenching sample when at 480°C
2G-34	Batch #7 (no In dopant)	840-845	125 (1.2 mm/hr)	96	60°C in 60 hr
2G-36	Batch #8	785			
2G-38	Batch #9	810	125 (1.2 mm/hr)	96	60°C in 75 hr



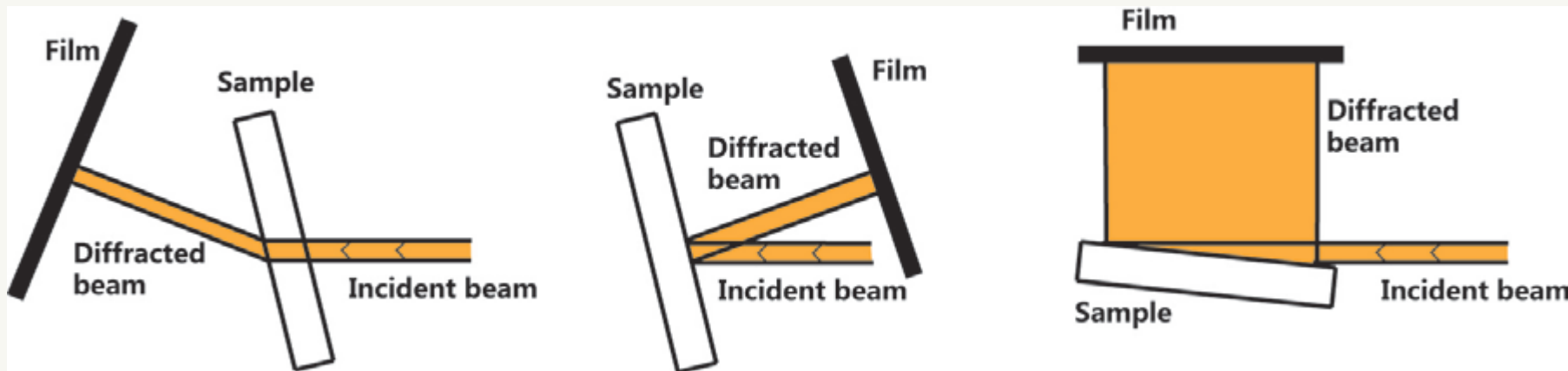
<http://alineason.com/index.php/en/knowhow/crystal-growth>

SYNCHROTRON X-RAY TOPOGRAPHY (SXRT)



NSLS X19C
White spectrum

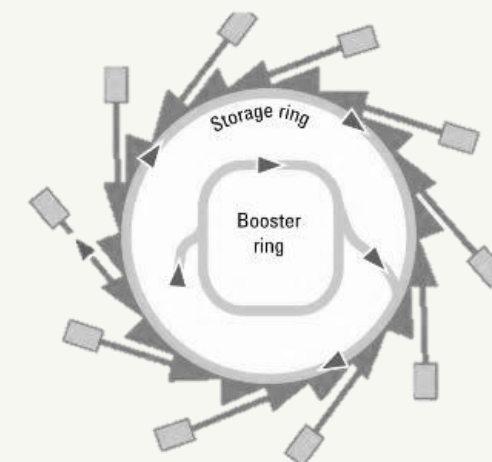
APS 1-BM
Monochromatic



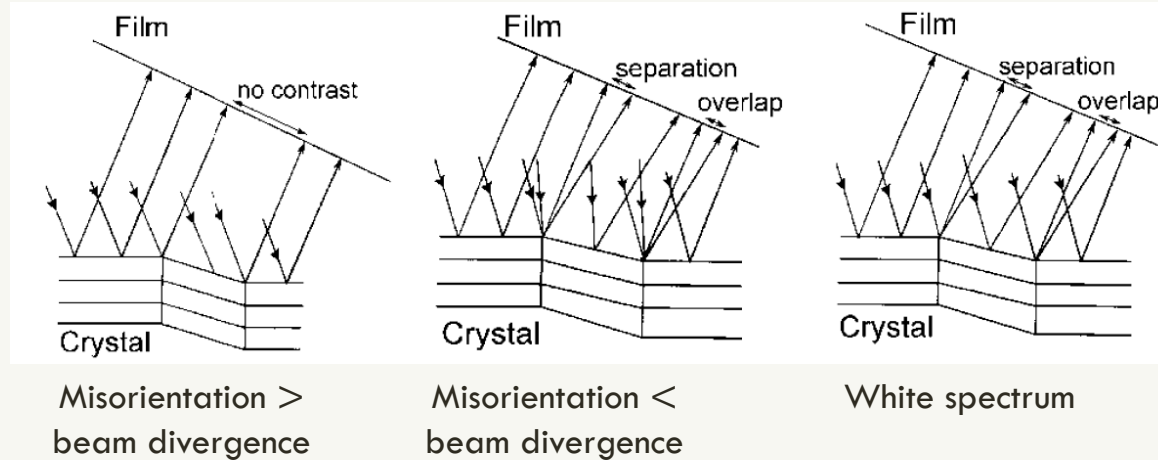
Transmission

Back-reflection

Grazing-incidence



CONTRAST FORMATION MECHANISM



Orientation contrast

Origin: misorientation leads to either the absence of diffracted beam or the overlapping/separation of diffracted beams, thus creating contrast.

Extinction contrast

- ❑ Direct image ($\mu t < 1-2$): waves diffracted from distorted region kinematically does not undergo primary extinction, thus having higher intensities than the waves from perfect regions.
- ❑ Intermediary image ($\mu t \sim 2-4$): new wavefields created at defect surface interference with original propagating wavefield creating fringe type contrast.
- ❑ Dynamic image ($\mu t > 5$): under high absorption condition, a small amount of deviation from the exact Bragg's condition will result in waves from branch 1 suffering much more absorption, leading to a white contrast.



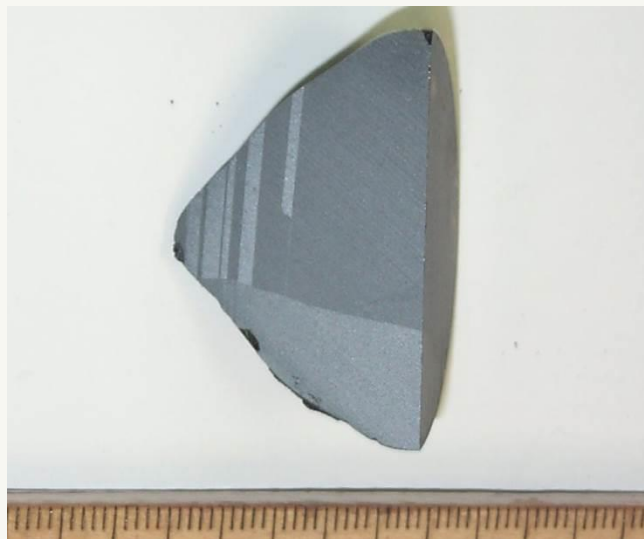
CORRELATION BETWEEN SYNCHROTRON WHITE BEAM X-RAY TOPOGRAPHY AND INFRARED MICROSCOPY



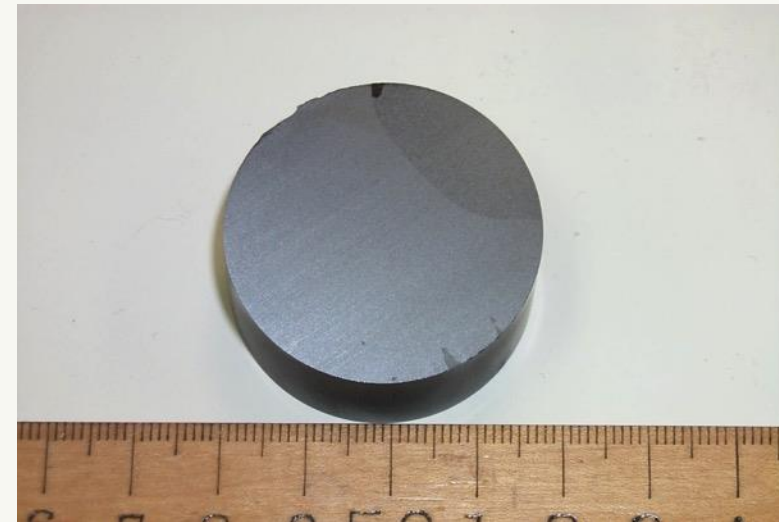
(a)



(b)



(c)

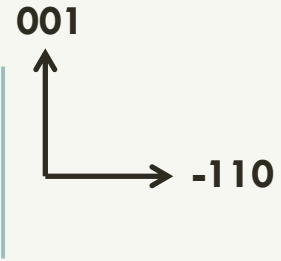


(d)

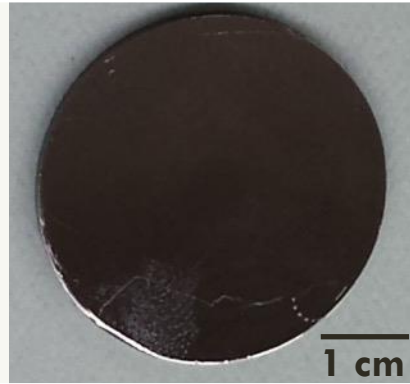
Pictures of a 38mm diameter grown crystal: (a) as-grown crystal slid inside ampoule (b) twins were observed at the tip shoulder (c) two grains were nucleated at the tip (d) two grains on a cutting surface with the major grain covers about 70% of the area.

CZT-36/1

X-ray topography



Photograph



Reflection SXRT

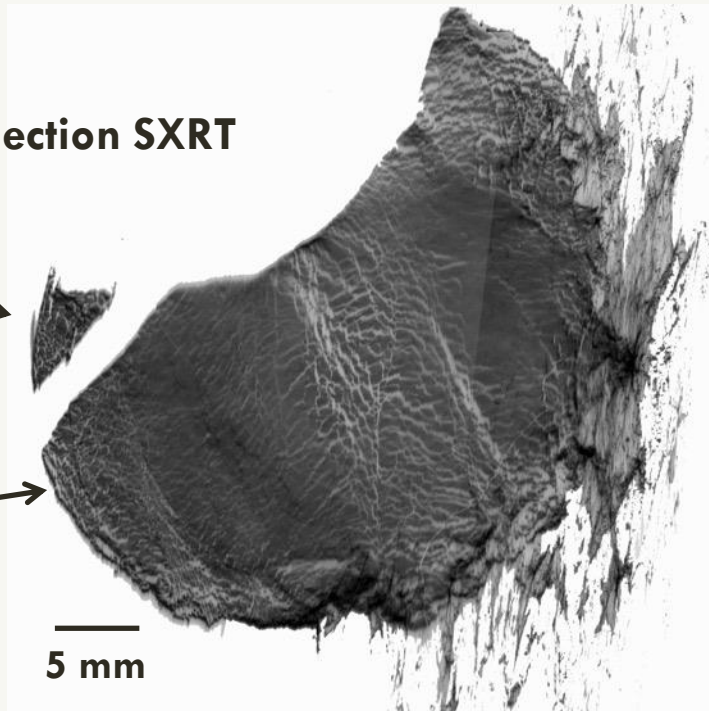
Grain 1



Grain 2

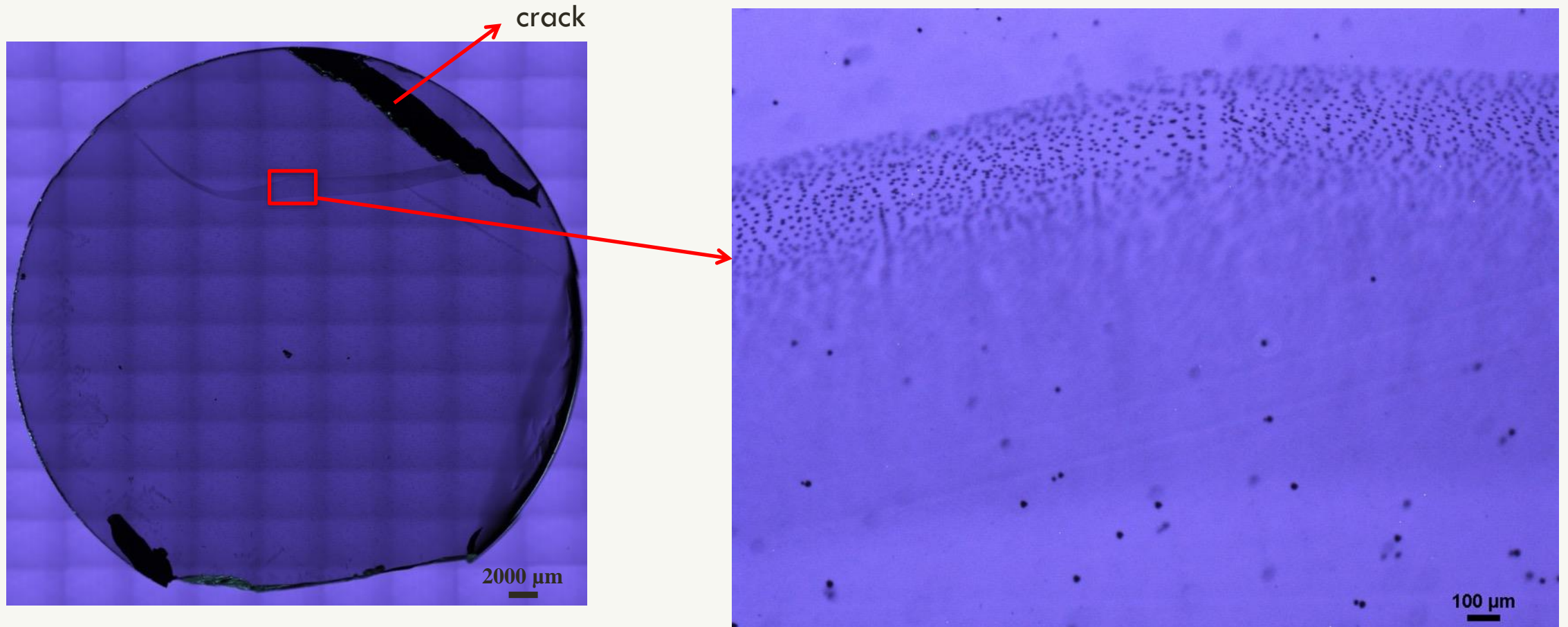


5 mm



- Sample CZT-36/1 was cut from CZT-36
- Reflection SXRT shows sample consists of two grain of relatively high crystallinity
- Network of subgrain boundaries and dislocation dominate the microstructure of the sample
- No precipitates are resolved on the topographs
- No slip bands or twins observed
- Relative lattice distortion near certain region along periphery most likely due to contact with ampoule walls

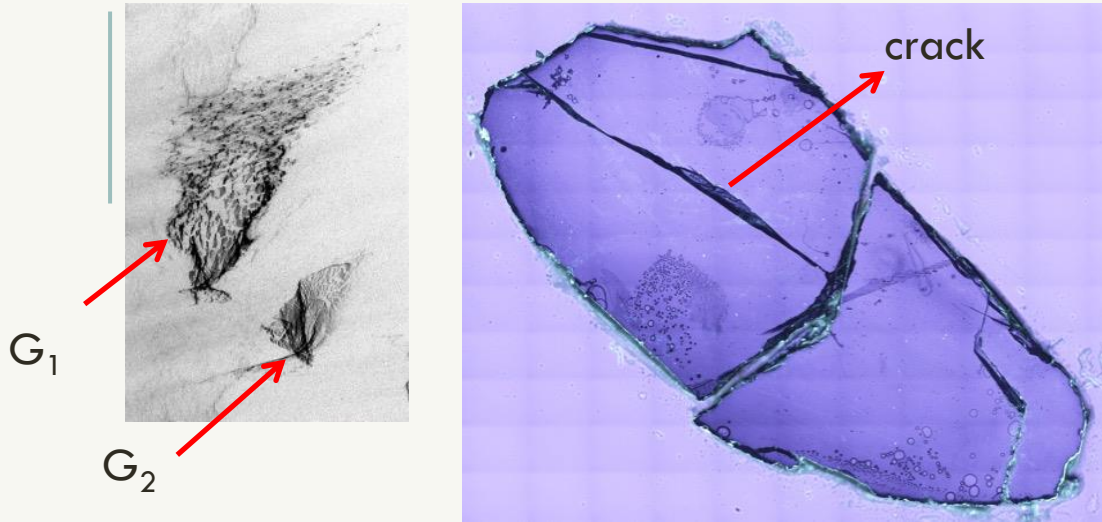
IR Microscopy



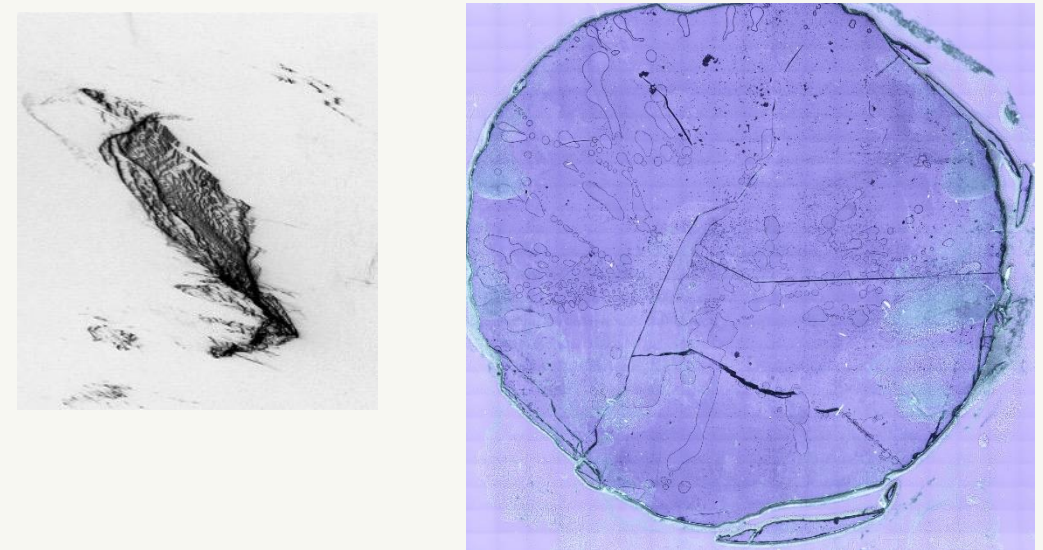
Left: Transmission infrared micrograph of CZT-36/1 showing crack, and a bed of Te inclusions inside a boundary

Right: Magnified I.R image of a section of Te filled boundary

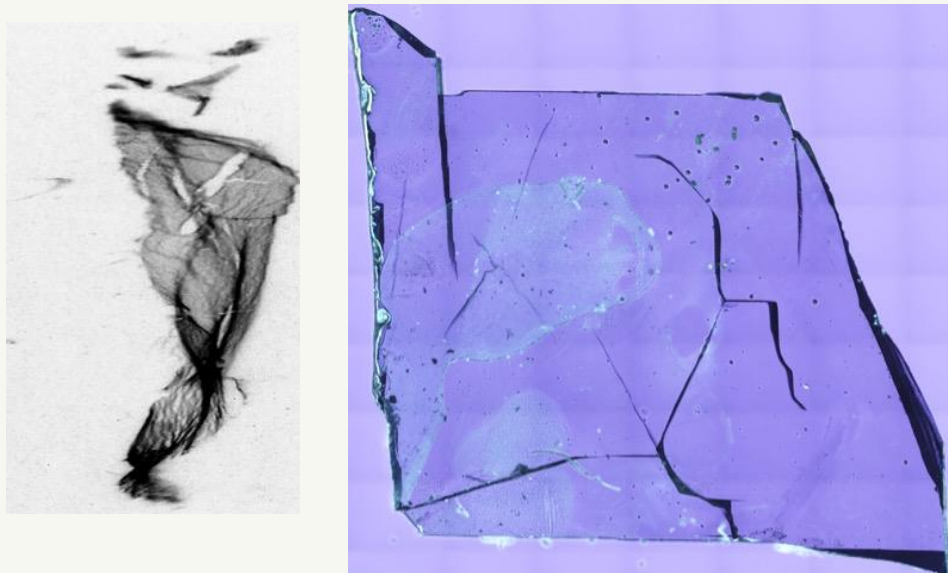
Sample 2G-30 @ 785°C



Sample 2G-31 @ 800°C



Sample 2G-34 @ 840-845°C

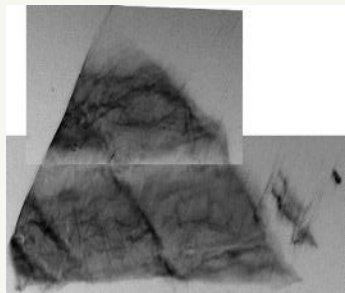


For each sample, left image is reflection SXRT of the whole sample, and right image is I.R micrograph of the sample

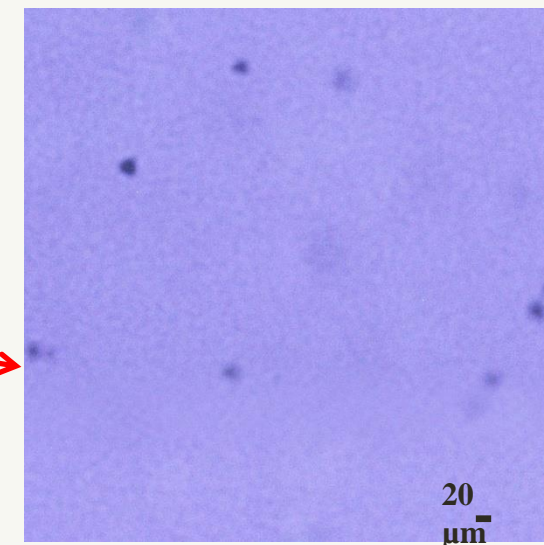
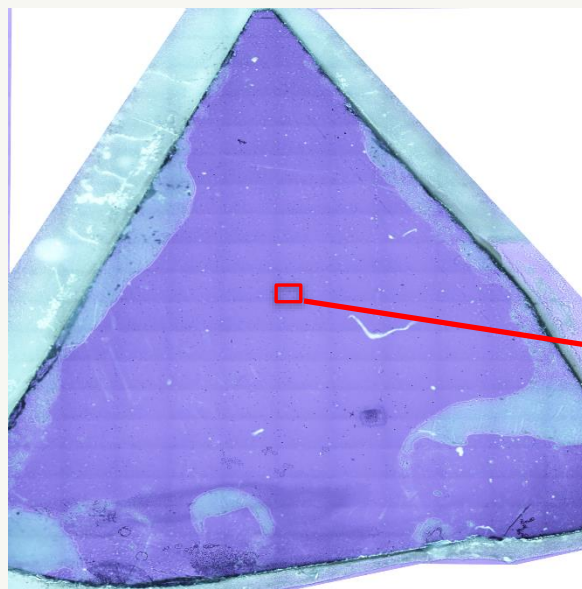
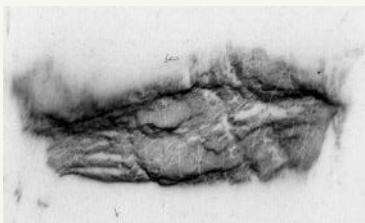
- Reflection SXRT reveals network of subgrain boundaries dominate the microstructure of samples
- Presence of inhomogeneous strain near edge of the samples
- G_1 in sample 2G-30 display the largest amount of strain
- I.R shows samples contains microcrack, which is can also cause the lattice distortion observed in the SXRT images

Sample 2G-36 @ 785°C

Transmission
SXRT



Reflection SXRT



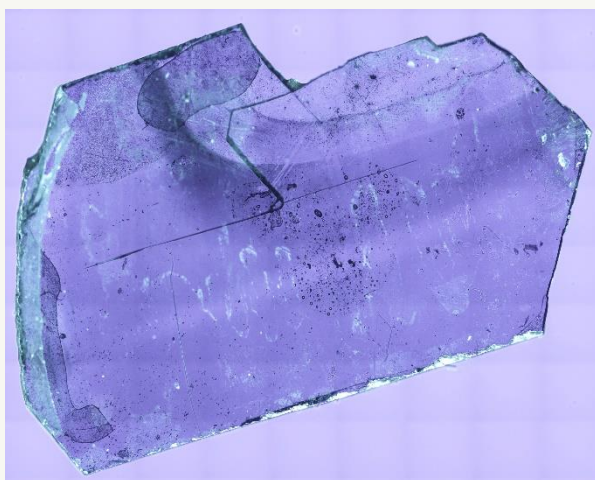
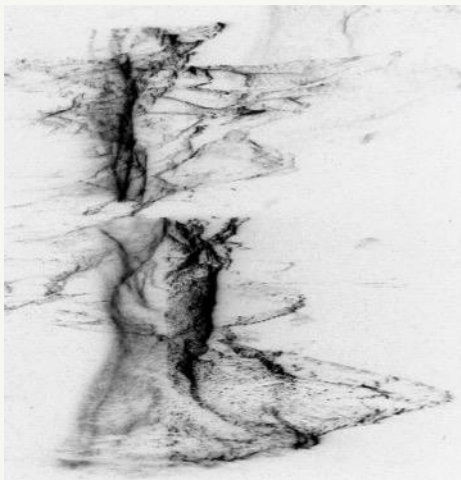
Sample 2G-36

- Both transmission and reflection indicate a single crystal, with a network of subgrain boundaries
- Lattice distortion near edges of sample due to inhomogeneous strain
- I.R. shows uniform distribution of Te inclusions smaller than 20 μm

Sample 2G-38

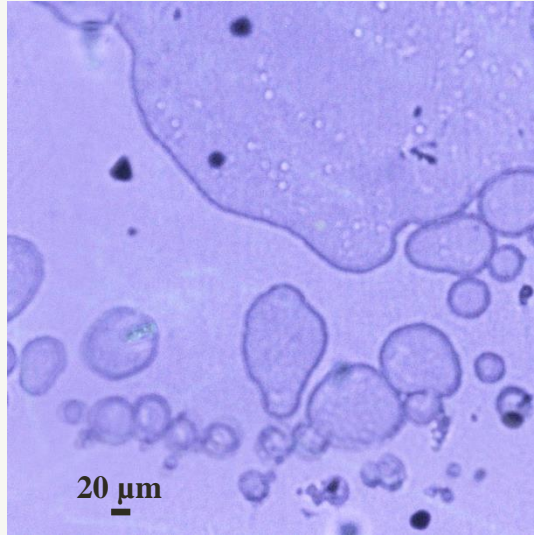
- Reflection SXRT shows a highly distorted image due to large inhomogeneous strain
- I.R. reveals the presence of microcrack, which also contributes to the lattice distortion observed in the SXRT images

Sample 2G-38 @ 810°C

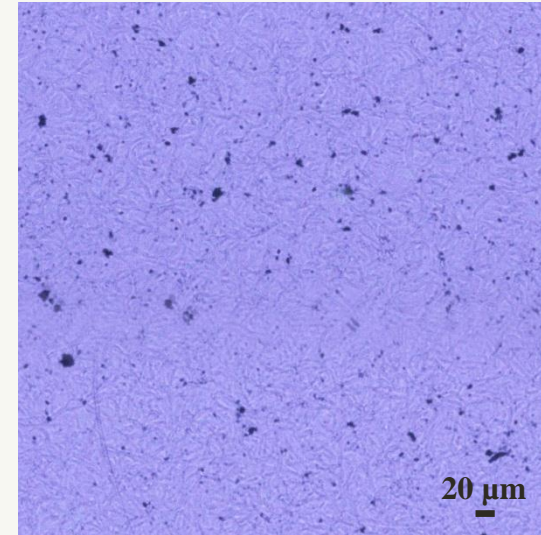


Enlarged I.R images showing size and shape of Te inclusions

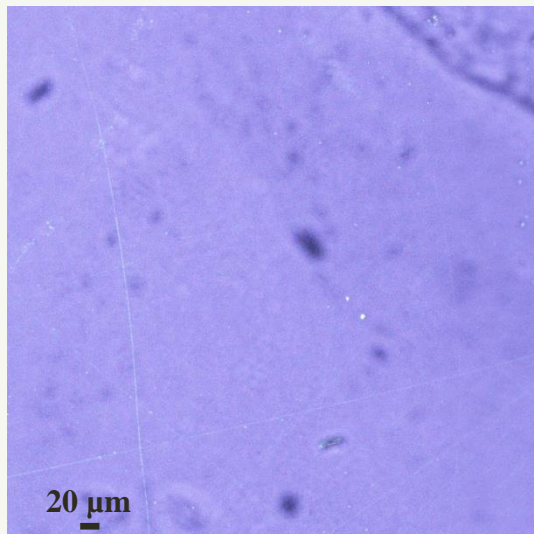
Sample 2G-30 @ 785°C



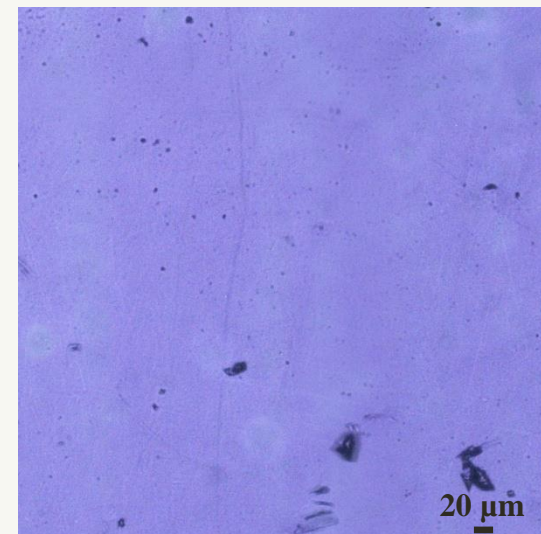
Sample 2G-31 @ 800°C



Sample 2G-34 @ 840-845°C

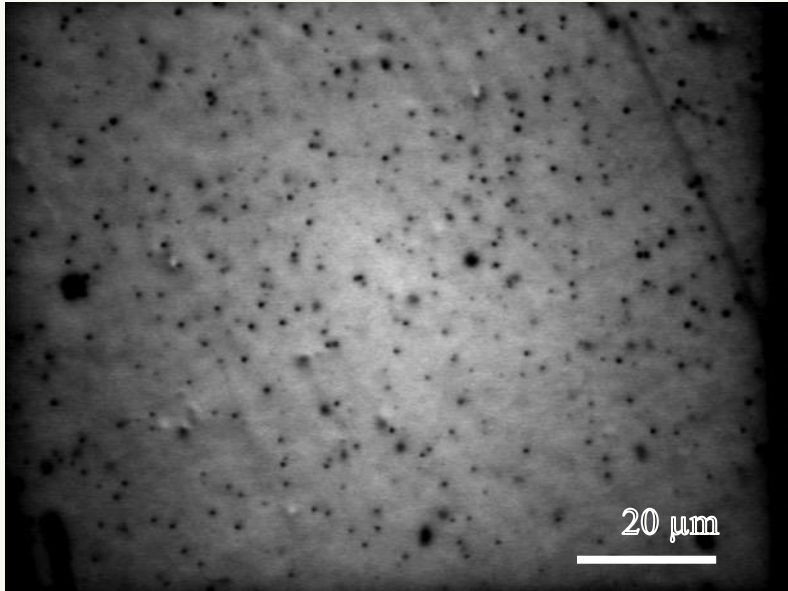


Sample 2G-38 @ 810°C

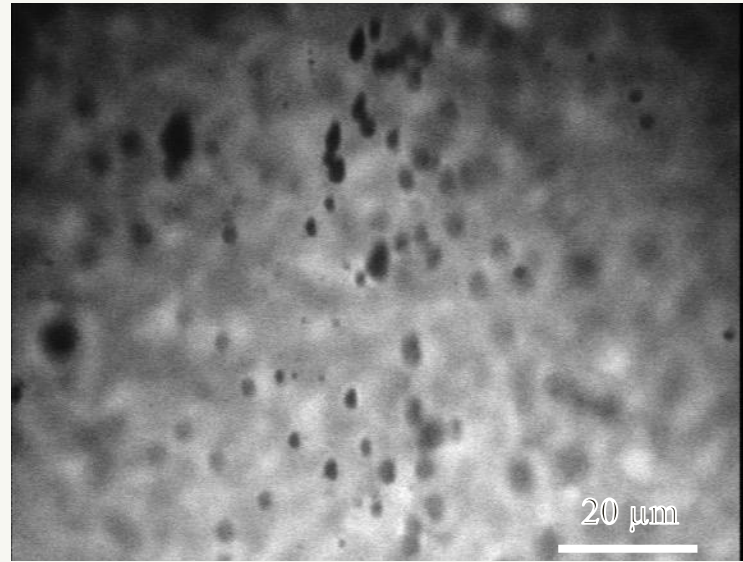




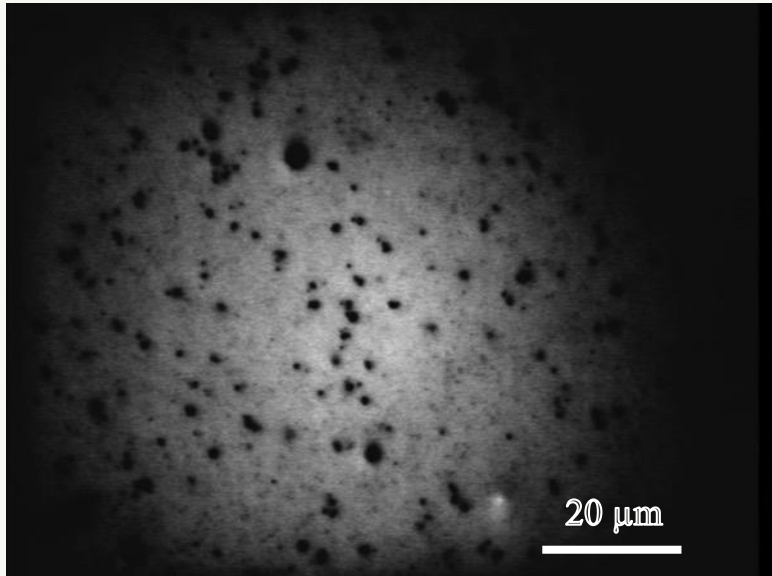
EFFECT OF C_d RESERVOIR TEMPERATURE ON T_e INCLUSIONS



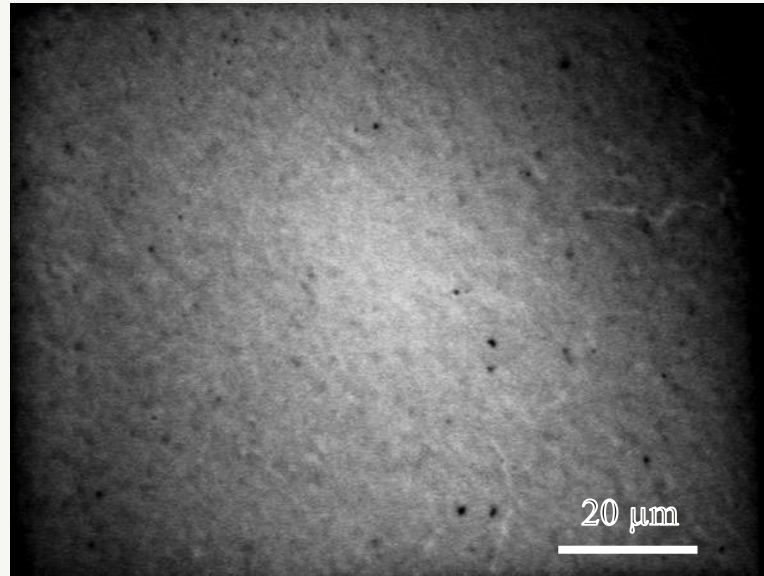
Cd reservoir temperature at 717°C



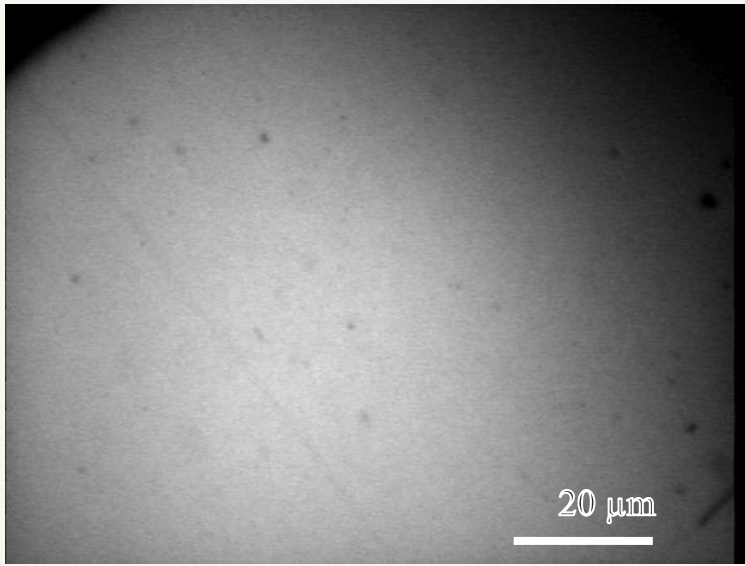
747°C



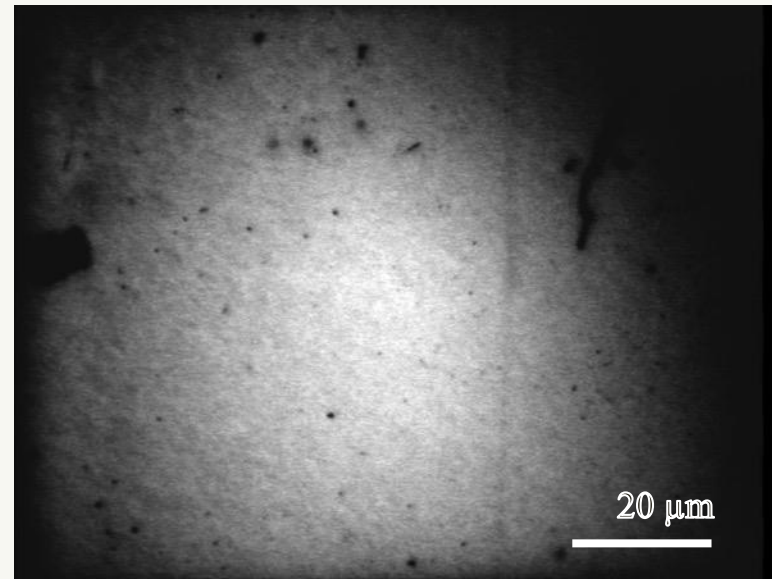
754°C



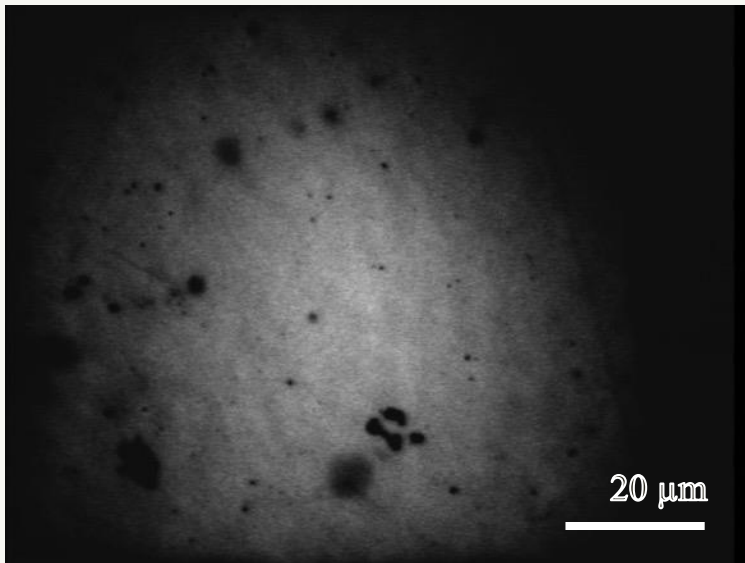
800°C



825°C



843°C



865°C

Lowest amount of precipitates were obtained with Cd reservoir temperature at $815 \pm 15^\circ\text{C}$ (comparing to 818°C predicted by partial pressure data for stoichiometric melt)

SUMMARY OF RESULTS

Sample #	Cd reservoir (°C)	Cd reservoir cooling rate	Twinning	Strain	Comments
2G-30	785	80°C in last 60hr	none	Severe lattice distortion near the edges, particularly in G ₁	Consists of 2 grains, with G1 showing a cellular microstructure and lattice distortion toward the edge
2G-31	800	65°C in last 60hr, quenching sample when sample at 480°C	none	Relatively small strain in main grain, with several highly distorted small grains	Single grain dominated by subgrain boundaries, and high density of dislocations.
2G-34	840-845	60°C in 60hr	none	Large distortion	Single grain, with relatively low strain dominated by subgrain boundaries and dislocation
2G-36	785		none	Very small strain near the edge	Single grain of good crystalline quality subgrain boundaries and low density of dislocation
2G-38	810	60°C in 75hr	none	Severe distortion due to large inhomogeneous strain	Single grain dominated by large inhomogeneous strain

ACKNOWLEDGMENT

- NASA/Marshall Space Flight Center for support and providing samples
- SWBXT work was carried out at Stony Brook Topography Facility (Beamline X19C) at the National Synchrotron Light Source (NSLS), Brookhaven National Laboratory (BNL) and 1-BM at Advanced Photon Source (APS), Argonne National Laboratory
- Anwar Hossain (BNL) for helping with the infrared microscopy measurements